The Track of the Pre-tRNA 5′ Leader in the Ribonuclease P Ribozyme−Substrate Complex†

Eric L. Christian and Michael E. Harris*

Center for RNA Molecular Biology, Department of Molecular Biology and Microbiology, Case Western Reserve University School of Medicine, Cleveland, Ohio 44106

Received June 4, 1999; Revised Manuscript Received July 19, 1999

ABSTRACT: The ribonuclease P (RNase P) ribozyme is an endonuclease that binds precursor tRNAs and catalyzes the removal of 5′ leader nucleotides. Biochemical and photo-cross-linking studies have identified sites of contact between the mature tRNA domain of pre-tRNA and the ribozyme; however, relatively little is known about the location of the 5′ leader in the ribozyme−substrate complex. To investigate the local three-dimensional environment of the 5′ leader, we employed the short-range photo-cross-linking agent 4-thiouridine (s^4U). The s^4U photoagent was incorporated into a series of pre-tRNA substrates containing unique uridine residues in the 5′ leader sequence at positions −1, −3, −5, −7, or −10. The modified substrates formed high-affinity complexes with the ribozyme and produced discrete intermolecular cross-links to RNase P RNA from *Bacillus subtilis.* Locations of the cross-linked nucleotides in the ribozyme and pre-tRNA were determined by reverse transcriptase primer extension. Photoagents incorporated into the 5′ leader detected discrete elements of ribozyme structure in a progression from J18/2 to L15 to P3. Importantly, all of the cross-linked species retained the ability to cleave the covalently attached pre-tRNA, indicating that the cross-links reflect the native structure of the ribozyme−substrate complex. Together with available structural and biochemical data, the cross-linking results suggest a model for the position of the 5′ leader within the ground-state ribozyme−substrate complex.

Ribonuclease P is a widespread and essential ribonucleoprotein enzyme that generates the mature 5′ ends of tRNAs via endonucleolytic cleavage. In bacteria, RNase P enzymes are generally heterodimers composed of a ca. 400 nucleotide RNA subunit and a small, but essential protein subunit of ca. 100 amino acids (reviewed in refs *1* and *2*). Many bacterial RNase P RNAs, however, retain the ability to bind pre-tRNAs and accomplish catalysis in the absence of the RNase P protein in vitro and so form one class of large ribozymes (*3*). Whereas Group I and Group II introns normally catalyze intramolecular self-splicing reactions, RNase P recognizes multiple RNA substrates in trans (*1, 2, 4*). Because the RNase P holoenzyme presumably recognizes all cellular pre-tRNAs, as well as other RNA substrates, it must be capable of identifying substrates which can differ in their primary sequence and secondary structure. It is therefore of significant interest to identify elements of RNase P RNA and pre-tRNA structure involved in substrate binding.

RNase P RNA contacts primarily the mature portion of pre-tRNA (*5*−*9*), through interactions involving functional groups in the acceptor stem and the T-stem and loop (*10*−*13*) (Figure 1). Deoxy substitutions of the 2′-hydroxyls at positions 54, 57, 61, and 62 and deletion of the 4-amino group of C56 in the T-loop result in significant decreases in the affinity of the ribozyme−substrate interaction (*11*−*13*). In addition, Pan and co-workers have provided evidence that the 2′-hydroxyl at position 62 interacts directly with nucleotide A233 in the P11 region of the *Bacillus subtilis* RNase P RNA (*11*) (Figure 1). Cross-linking, chemical protection, and kinetic data also show that the conserved 3′ CCA sequence of bacterial tRNAs interacts with a loop or internal bulge located at helix P15 (*14, 15*). Kirsebom and colleagues demonstrated that this interaction involves base pairing between the C residues at positions 74 and 75 in tRNA and two specific guanosines in L15 of RNase P RNA (*16*) (Figure 1). Not only is the P15−CCA interaction important for aligning the substrate phosphate for cleavage, but it also likely assists in positioning divalent metal ions important for catalysis (*17*).

Functional groups on the ribozyme involved in substrate recognition have been identified using nucleotide analogue interference mapping (*18*−*21*). Importantly, these nucleotide positions overlap with regions identified as being adjacent to the bound substrate by intermolecular cross-linking experiments (*22*−*26*). These regions include conserved adenosines in J5/15 that are in close proximity to the pre-tRNA cleavage site, P11 and P9 which are involved in contacting the T-stem and loop, and J18/2 which may be involved in recognition of the proximal portion of the 5′ leader (Figure 1). Individual functional groups in J11/12 may also play a role in substrate binding (*20, 21, 27*); however, it is not yet clear whether this region directly contacts the pre-tRNA. Interestingly, the highly conserved helix P4, which has been proposed to play a direct role in substrate recognition and catalysis, has not been detected with intermolecular photo-cross-linking approaches (*18, 24*−*26, 28*−*30*).

† This research was supported by a pilot study grant from the American Cancer Society (IRG-186B) and a grant from the NIH (GM56740) to M.E.H.

* Corresponding author: e-mail, meh2@pop.cwru.edu; phone, 216-368-4779; fax, 216-368-3055.

10.1021/bi991278a CCC: $18.00
Published on Web 09/09/1999

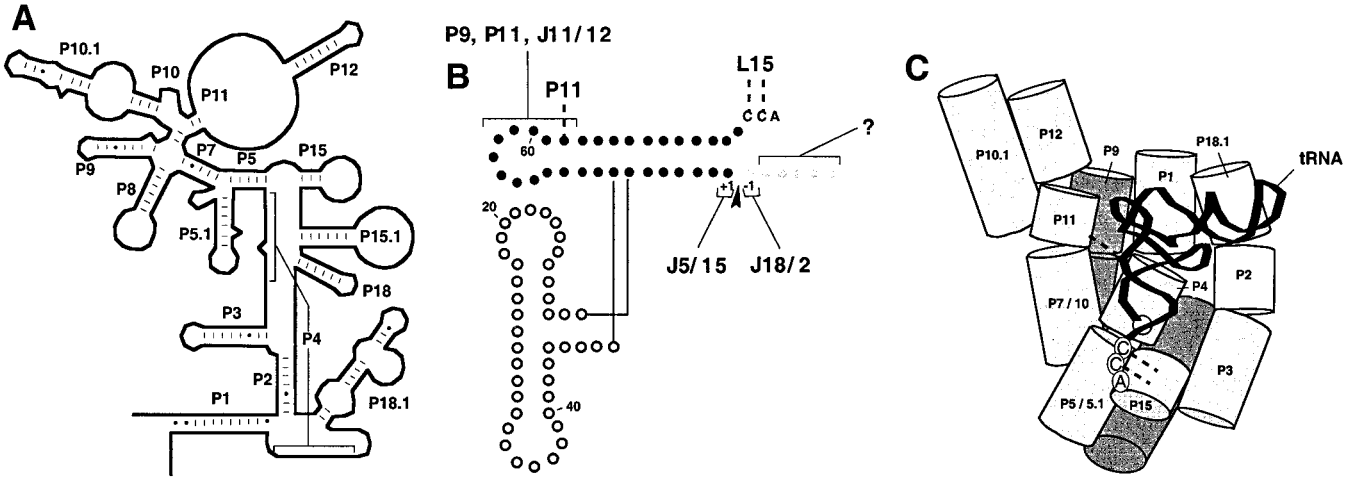

FIGURE 1: Secondary and proposed tertiary structure of the RNase P ribozyme−substrate complex. (A) Secondary structure of *B. subtilis* RNase P RNA. The nomenclature for the RNase P RNA secondary structure is from Haas et al. (*47*). Helices are numbered from the 5′ end and given the designation P (paired). Regions joining helices are given the designation J (joining) and numbered according to the helices that they connect (i.e., J3/4 connects helices P3 and P4). Nucleotides forming helix P4 are indicated with brackets. (B) Secondary structure of pre-tRNA. The acceptor and T-stem portions that are primarily involved in recognition by RNase P RNA are shown as filled circles, the anticodon stem and the D-stem are shown as open circles, and the 5′ leader is shown as gray circles. The RNase P cleavage site is indicated by an arrowhead. Locations of sites of interaction with RNase P RNA are shown by dashed lines. Elements of ribozyme structure detected by cross-linking that are in the vicinity of the bound substrate are indicated by brackets. (C) Illustration of helix positions in a model of the *B. subtilis* ribozyme−substrate complex (*25, 34*). Positions and orientations of helices are shown as cylinders labeled according to panel A. The phosphodiester backbone of the bound tRNA is shown as a ribbon. The interactions between RNase P RNA and tRNA discussed in the text and shown in panel B are indicated by dashed lines.

In contrast to the RNA−RNA interactions between the mature domain of the pre-tRNA substrate and the ribozyme, relatively little is known about the recognition of the 5′ leader by RNase P RNA. There is evidence to suggest that both RNA and protein might contact substrate RNA sequences upstream of the cleavage site. RNase P protein from *B. subtilis* alters the substrate specificity of the ribozyme by enhancing the affinity for pre-tRNA, and comparisons of the binding affinities of substrates with different leader lengths indicate that recognition occurs via interactions with nucleotides −2 to −5 of the 5′ leader (*31*). The protein-dependent recognition of the pre-tRNA leader could be the result of direct contacts between the substrate and the protein or may be mediated by protein-induced conformational changes in the RNA. Consistent with the first possibility, photo-cross-linking and biochemical studies indicate that a significant part of the enhanced substrate affinity is due to direct contacts between the 5′ leader and the protein subunit (*32*).

In addition to the protein interface with the 5′ leader, there is biochemical evidence for direct contacts between the J18/2 region of the ribozyme and these sequences. Nucleotide bases in J18/2 are protected from chemical modification by pre-tRNA, but not tRNA (*14*), and photo-cross-linking has been reported between J18/2 and the proximal portion of the 5′ leader (*24*). In addition, we recently detected short-range photo-cross-links between J18/2 and a 6-thioguanosine at the 5′ end of a pre-tRNA substrate with a single nucleotide leader sequence, indicating that J18/2 is positioned immediately adjacent to the cleavage site (*26*). To build on these short-range cross-linking studies, we set out to determine whether more distal elements of the 5′ leader are associated with discrete elements of ribozyme structure.

Here, we report photo-cross-linking results which position the 5′ leader within the ground-state ribozyme−substrate complex. The *B. subtilis* RNase P RNA was chosen for study in this analysis since much of the effort directed at understanding 5′ leader recognition has involved this ribozyme (e.g., ref *11*−*15*, *31*, and *32*). We detect specific cross-links between 4-thiouridine (s^4U) residues at positions −1, −3, −5, −7, and −10 in the pre-tRNA 5′ leader sequence and discrete elements of ribozyme structure. In addition to confirming that J18/2 is in close proximity to the nucleotides at positions −1 and −3 in the 5′ leader, these results show that nucleotides at positions −5 and −7 are adjacent to the CCA binding site in L15. Furthermore, we find that the −10 position cross-links to both L15 and P3, which have recently been shown to be in proximity in the folded ribozyme (*25, 33*). In the context of recent structural models of the ribozyme−substrate complex (*25, 34*), these cross-linking results indicate a specific track for the 5′ leader on the surface of the ribozyme−substrate complex.

MATERIALS AND METHODS

RNA Synthesis and Purification. B. subtilis RNase P RNA and *B. subtilis* pre-$tRNA^{Asp}$ were generated by in vitro transcription from linearized plasmids as described previously (*26*). Pre-tRNA genes for in vitro transcription were generated by PCR amplification from the wild-type pre-$tRNA^{Asp}$ template (pDW152). Specifically, DNAs for the transcription of the L[0], L[−1], L[−3], L[−5], L[−7], and L[−10] substrates were generated from pairwise combinations of "reverse" oligonucleotide primer PT-T-R (CGGGATCCTG-GCAGTCCGGAC) containing a *Bam*HI restriction site and sequences complementary to the 3′ end of *B. subtilis* pre-$tRNA^{Asp}$ and a "forward" oligonucleotide primer containing an *Eco*RI site flanking sequences corresponding to the 5′ leader and the 5′ portion of *B. subtilis* $tRNA^{Asp}$. "Forward" oligonucleotide primers TXNOUF (GGAATTCTAATAC-GACTCACTATAGGGCACGGAACCCAAAAAGGTCC-GG), TXU1F (GGAATTCTAATACGACTCACTATAG-GGCACGGAACCCAAAATGGTCCGG), TXU3F (GG-AATTCTAATACGACTCACTATAGGGCACGGAACCCAATA-

AGGTCCGG), TXU5F (GGAATTCTAATACGACTCACTATAGGGCACGGAACCCTAAAAGGTCCGG), TXU7F (GGAATTCTAATACGACTCACTATAGGGCACGGAACTCAAAAAGGTCCGG), and TXU10F (GGAATTCTAATACGACTCACTATAGGGCACGGTACACAAAAAGGTCCGG) were used to generate substrates with no uridine in the 5′ leader sequence or unique uridine residues at position −1, −3, −5, −7, or −10 in the 5′ leader sequence, respectively. PCR-amplified fragments were separated on 2% agarose and extracted by centrifugation through a 0.45 μm Durapore membrane (Millipore). PCR fragments were phenol extracted twice in equal volumes of a 1:1 mixture of phenol and chloroform and once with an equal volume of chloroform and subsequently recovered by precipitation in 0.3 M sodium acetate and 3 volumes of ethanol. PCR fragments were then digested with *Eco*RI and *Bam*HI (New England Biolabs), phenol extracted, and ethanol precipitated as described above. The digested PCR fragments were then ligated into pUC18 plasmids previously digested with *Eco*RI and *Bam*HI.

Pre-tRNA substrates were produced by transcribing 2 μg of plasmid template in the presence of transcription buffer containing 40 mM Tris-HCl, pH 7.9, 6 mM $MgCl_2$, 2 mM spermidine, 10 mM dithiothreitol, 6 mM guanosine, 1 mM each ATP, CTP, and GTP, and 0.1 mM each UTP and s^4UTP (USB) in a total volume of 100 μL at 37 °C overnight with 40 units of T7 RNA polymerase. Transcription reactions were terminated by dilution to 200 μL with 10 mM Tris-HCl, pH 8.0, and 1 mM EDTA, followed by precipitation in 0.3 M sodium acetate and 3 volumes of ethanol. Transcripts were resolved on a 6% (19:1) polyacrylamide gel (National Diagnostics). Individual RNA bands were visualized by UV shadowing, excised, and eluted overnight in 0.3 M sodium acetate, 10 mM Tris-HCL, pH 8.0, 1 mM EDTA, and 0.1% SDS. The eluted RNAs were phenol extracted and recovered by ethanol precipitation. RNA concentrations and level of 4-thiouridine incorporation were measured by absorbance at 260 and 331 nm, respectively. A ϵ_{331} of 21.2×10^{-3} was used for s^4U-containing RNAs. Transcripts (20 pmol) were subsequently 5′ end-labeled for binding and cross-linking studies with 150 μCi of [γ-^{32}P] ATP (New England Nuclear) and T4 polynucleotide kinase (Life Sciences).

Measurement of Binding Affinities. The binding affinity of the L[0], L[−1], L[−3], L[−5], L[−7], and L[−10] substrates to *B. subtilis* RNase P RNA was measured by a gel filtration method adapted from Beebe and Fierke (*35*) and used in previous studies involving modified cross-linking substrates (*26*). 5′-^{32}P end-labeled pre-tRNA substrates in 300 μL were renatured separately from unlabeled *B. subtilis* RNase P RNA (20 μL samples at concentrations of 0, 2.5, 5, 10, 20, 30, 40, 60, 100, 200, 300, and 400 nM) in 2 M ammonium acetate, 40 mM Tris-HCl, pH 8.0, 0.05% NP-40, and 25 mM $CaCl_2$ by incubation at 65 °C for 3 min followed by incubation at 37 °C for 20 min. Aliquots (20 μL) of renatured pre-tRNA substrates at 2.5 nM were combined with renatured samples of *B. subtilis* RNase P RNA and allowed to incubate for an additional 2 min at 37 °C. Ribozyme−substrate complexes were separated from unbound pre-tRNA substrates by size-exclusion chromatography using G-75 Sephadex. Samples were spun for 1.5 min at 1000*g* through 0.6 mL of G-75 Sephadex (Pharmacia) packed in Bio-Spin columns (Bio-Rad) preequilibrated in 2 M ammonium acetate, 40 mM Tris-HCl, pH 8.0, 25 mM $CaCl_2$, and 0.05% NP-40. The extent of ribozyme−substrate complex formation was determined by Cerenkov scintillation counting of the excluded volume. The dissociation constant (K_d) was derived by plotting the fraction of bound substrate versus enzyme concentration and fitting the data to the equation

$$[E-S]/[E-S]_\infty = 1/\{1 + (K_d/[E])\} \quad (1)$$

where [E−S] is the amount of radioactivity measured in the flow-through, $[E-S]_\infty$ is the maximum amount of bound radioactive substrate at the highest ribozyme concentrations, and [E] is the concentration of ribozyme.

Photo-Cross-Linking and Isolation of Cross-Linked Species. Cross-linking was done under conditions of excess *B. subtilis* ribozyme ([E]/[S] = 10) in the presence of $CaCl_2$ to maximize binding and suppress catalysis during the cross-linking reaction (*36*). Transcription reactions and cross-linking experiments were done in amber microfuge tubes (Fisher, no. 05-470-15). All operations involving s^4UTP and s^4U-modified RNA were performed in low ambient light conditions to minimize premature activation of the photoagent. Pre-tRNAs containing, on average, one 4-thiouridine per molecule and unmodified *B. subtilis* RNase P RNA were initially resuspended separately to a concentration of 100 nM and 1 μM, respectively, in 2 M ammonium acetate, 50 mM Tris-HCl, pH 8.0, and 25 mM $CaCl_2$. The RNAs were renatured by heating to 65 °C for 3 min followed by incubation at 37 °C for an additional 20 min. Prior to cross-linking, equal volumes (200 μL) of pre-tRNAs and *B. subtilis* ribozyme were mixed and allowed to bind at 37 °C for 2 min and then placed on ice. The entire sample was placed on a parafilm-covered aluminum block on ice in 12 μL aliquots. The samples were irradiated at 366 nm (using a Model UVGL-58 Mineralight lamp manufactured by UVP, Upland, CA) for 15 min through a $^1/_8$ in. glass plate at a distance of 3 cm (*22*). Individual aliquots were then pooled and phenol extracted, and the RNA was recovered by ethanol precipitation. Cross-linked RNAs were separated from uncross-linked material on a 4% (19:1) polyacrylamide gel and recovered as described above but with the addition of 1 mg/mL glycogen to facilitate precipitation.

Mapping of Cross-Linked Nucleotides and Determination of Catalytic Activity. The positions of individual pre-tRNA−RNase P RNA cross-links were determined by primer extension (*22*). For primer extension analysis of RNase P RNA the following oligonucleotides were used: BS182 (GAGACTTCGTCACTGTGGC), BS384 (AAGTGGTCTAACGTTCTGTAAG), and BS81 (CTTCGCTAGGCACGAACACTACG). For primer extension analysis of pre-$tRNA^{Asp}$ sequences the oligonucleotide 3′TASP (TGGCGGTCCGGACGGGAC) was used. Specifically, 0.2 pmol of 5′-^{32}P end-labeled sequencing primer complementary to either RNase P RNA or tRNA was annealed to 0.05−0.2 pmol of cross-linked material in a total volume of 5 μL at 65 °C for 3 min in 50 mM Tris-HCl, pH 8.3, 15 mM NaCl, and 10 mM dithiothreitol and set immediately on dry ice. Samples were thawed on ice and $MgCl_2$ (1 μL) was added to a final concentration of 6 mM, followed by the addition of each of the four deoxynucleotides (dATP, dCTP, dGTP, dTTP) to a final concentration 400 μM. Reactions (8 μL) were initiated by the addition of 2 units (2 μL) of AMV reverse tran-

scriptase (Boehringer Mannheim) and then incubated at 47 °C for 5 min. Reactions were then quenched by the addition of an equal volume of 0.5 M NaCl, 20 mM EDTA, and 0.5 μg of glycogen (Boehringer Mannheim) and precipitated in 2.5 volumes of ethanol. Primer extension products were resuspended in 2 μL of distilled H_2O and denatured in the presence of an equal volume of gel loading buffer (95% formamide, 150 mM Tris-HCl, pH 8.0, 15 mM EDTA, 1 mg/mL each bromphenol blue and xylene cyanol FF), heated for 3 min at 95 °C, and allowed to cool on ice before being loaded (2 μL) onto a 6% (19:1) polyacrylamide gel adjacent to standard dideoxy sequencing reactions of un-cross-linked *B. subtilis* RNase P RNA as described previously (*26*).

Gel-purified cross-linked species were analyzed for their ability to undergo catalysis by incubation in the presence of 2 M ammonium acetate, 50 mM Tris-HCl, pH 8.0, and 25 mM $MgCl_2$ for 60 min at 37 °C. Reactions were subsequently phenol extracted and the RNAs recovered by ethanol precipitation as described above and separated on a 6% (19:1) polyacrylamide gel adjacent to unreacted controls.

RESULTS

Intermolecular Cross-Linking between s^{4}U-Modified Pre-tRNA and RNase P RNA. To examine the position of the 5′ leader in the bacterial RNase P ribozyme−substrate complex and to build upon previous studies of the position of nucleotides at the pre-tRNA cleavage site, the photoaffinity agent s^{4}U was incorporated into pre-tRNA substrates by in vitro transcription and cross-linked to *B. subtilis* RNase P RNA. s^{4}U contains a sulfur in place of the carbonyl oxygen at position 4 in the uridine base (Figure 2A). This nucleotide analogue is a useful short-range (2−3 Å) cross-linking reagent and has been frequently employed to investigate RNA−RNA and RNA−protein interactions (e.g., refs 37−39). Illumination of s^{4}U with long-wave UV light results in the formation of a s^{4}U radical species which is highly reactive and can insert into covalent bonds or react with alcohols and amines that are in close proximity (*40*).

To determine the level of s^{4}U incorporation during transcription, we took advantage of the fact that substitution with sulfur at the O4 position of the uridine base results in absorption at 331 nm (*41*). Since the four standard nucleotide bases do not absorb significantly at this wavelength, A_{331} is a direct measure of the concentration of s^{4}U. By monitoring the absorbance at 331 nm of pre-tRNAs transcribed in vitro, the relative levels of s^{4}U and UTP in transcription reactions could be adjusted to produce a population of pre-tRNAs containing, on average, a single s^{4}U residue per molecule and thus diminishing the complication of analyzing multiple cross-linked species.

Because the sequence of the 5′ leader varies significantly in vivo and there are no consistent sequence preferences for substrate binding (*42*), we manipulated the 5′ leader sequence to alter the position of incorporation of s^{4}U residues in the 5′ leader and simplify the cross-linking analysis. Specifically, we developed a series of five pre-tRNA substrates with individual uridines at discrete positions relative to the cleavage site (Figure 2B). Pre-tRNA substrates L[−1], L[−3], L[−5], L[−7], and L[−10] have unique uridine residues at positions −1, −3, −5, −7, and −10 in the 5′ leader sequence, respectively. In addition, a control substrate,

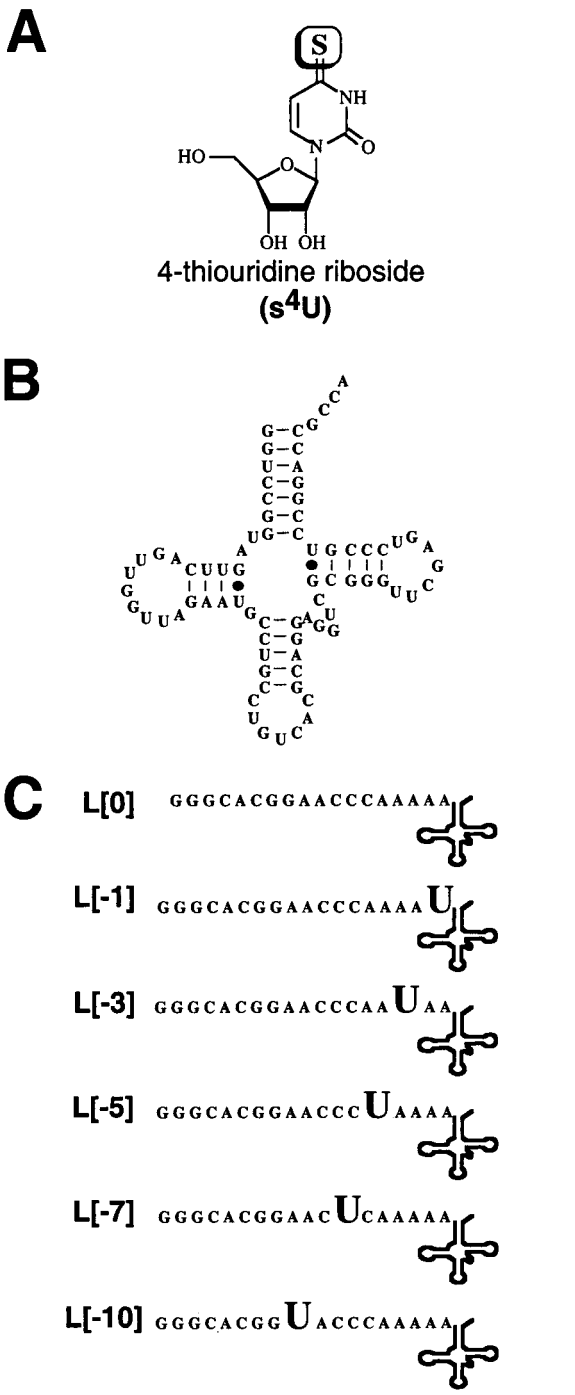

FIGURE 2: (A) Structure of 4-thiouridine. The substitution of the carbonyl oxygen at position 4 by sulfur is highlighted. (B) Sequence and secondary structure of *B. subtilis* tRNA^{Asp}. (C) Sequences of the 5′ leaders of substrates L[0], L[−1], L[−3], L[−5], L[−7], and L[−10].

L[0], containing no uridines in the 5′ leader sequence was constructed to distinguish cross-linking contacts to the mature tRNA domain.

We first determined the ability of the L[0], L[−1], L[−3], L[−5], L[−7], and L[−10] substrates to form high-affinity complexes with the ribozyme. The dissociation constants for the binding interaction between these substrates and the ribozyme were determined by gel filtration as described in Materials and Methods (Table 1). Briefly, 5′-^{32}P end-labeled pre-tRNA precursors were bound to *B. subtilis* RNase P RNA over a range of ribozyme concentrations in reaction buffer

Table 1: Binding Constants and Sites of Intermolecular Cross-Linking for Pre-tRNA Substrates

substrate	K_d (nM)[a]	cross-linked species	cross-linked nucleotides
pre-tRNA^{Asp}	14.8 ± 3.6	N/A	N/A
L[0]	16.7 ± 3.8	N/A	N/A
L[−1]	19.6 ± 5.7	L[−1]a	A318, G319 (J18/2)
L[−3]	15.9 ± 3.6	L[−3]a	A245, A246 (J5/15)
		L[−3]b	U317, A318, G319 (J18/2)
L[−5]	21.5 ± 5.8	L[−5]a	G258, G259 (L15)
		L[−5]b	A320 (J18/2)
L[−7]	12.8 ± 3.1	L[−7]a	G259, U260, A261 (L15)
L[−10]	13.9 ± 3.9	L[−10]a	G258, G259, U260, A261 (L15)
		L[−10]b	A36, U37 (P3)

[a] Dissociation constants (K_d) were determined by gel filtration through G-75 Sephadex in 2 M ammonium acetate, 50 mM Tris-HCl, pH 8.0, 25 mM calcium chloride, and 0.01% NP-40.

containing 25 mM $CaCl_2$ which allows binding of the pre-tRNA substrate but significantly slows the catalytic rate (*36*). The extent of ribozyme−substrate complex formation was measured as the level of radioactivity in the excluded volume. Under these conditions, the *B. subtilis* pre-tRNA^{Asp} binds to the ribozyme with a K_d of ca. 15 nM while the L[0], L[−1], L[−3], L[−5], L[−7], and L[−10] substrates bind with K_d values ranging from ca. 13 to 22 nM (Table 1). In addition, all of the substrates were found to be accurately and efficiently cleaved by the ribozyme (data not shown). Thus, consistent with the phylogenetic data, sequence changes introduced into the 5′ leader of pre-tRNAs used in the current study have only modest effects on substrate binding and activity. Therefore, they are likely to form equivalent structures within the ribozyme−substrate complex.

s^{4}U-modified pre-tRNA substrates were next cross-linked to *B. subtilis* RNase P RNA under the same conditions used for the binding analysis. Irradiation of radiolabeled s^{4}U-modified pre-tRNAs in the presence of RNase P RNA results in the formation of slower mobility species consistent with intermolecular cross-links (Figure 3A). Formation of these species requires irradiation with the appropriate wavelength of UV light and use of s^{4}U-modified pre-tRNA. No cross-linked species were observed using unmodified pre-tRNA or in the absence of either RNase P RNA or UV irradiation (Figure 3 and data not shown). These data indicate that the products represent intermolecular cross-links between the photoagent-modified pre-tRNA and RNase P RNA.

The L[0] substrate, which lacks uridine residues in the leader portion of the RNA, forms only two cross-links (Figure 3): a slowly migrating band we designate L[0]a, and a faster migrating species designated L[0]b. In contrast, the L[−1] substrate, which contains a single uridine in the 5′ leader sequence at the −1 position, forms an additional intermolecular cross-link (labeled L[−1]a in Figure 3B) that is not formed using the L[0] RNA. Likewise, the L[−3], L[−5], L[−7], and L[−10] substrates, which contain single uridine residues in the 5′ leader sequence at positions −3,−5,−7, and −10, respectively, form the cross-links seen with the L[0] RNA but also produce unique cross-links. In fact, the cross-linked species obtained with L[−5], L[−7], and L[−10] are of such high efficiency that the lower efficiency cross-links which correspond to those observed with L[0] are difficult to visualize on the longer exposure shown in Figure 3A. Shorter exposures allowed the identification of an additional band involving L[−5] (L[−5]b) running just below the major cross-linked species seen in Figure 3B. The cross-linked species obtained with the L[−1], L[−3], L[−5], L[−7], and L[−10] substrates but not with the L[0] RNA are thus likely to have resulted from intermolecular cross-linking between the unique uridine residues in the 5′ leader sequences of these substrates and the ribozyme.

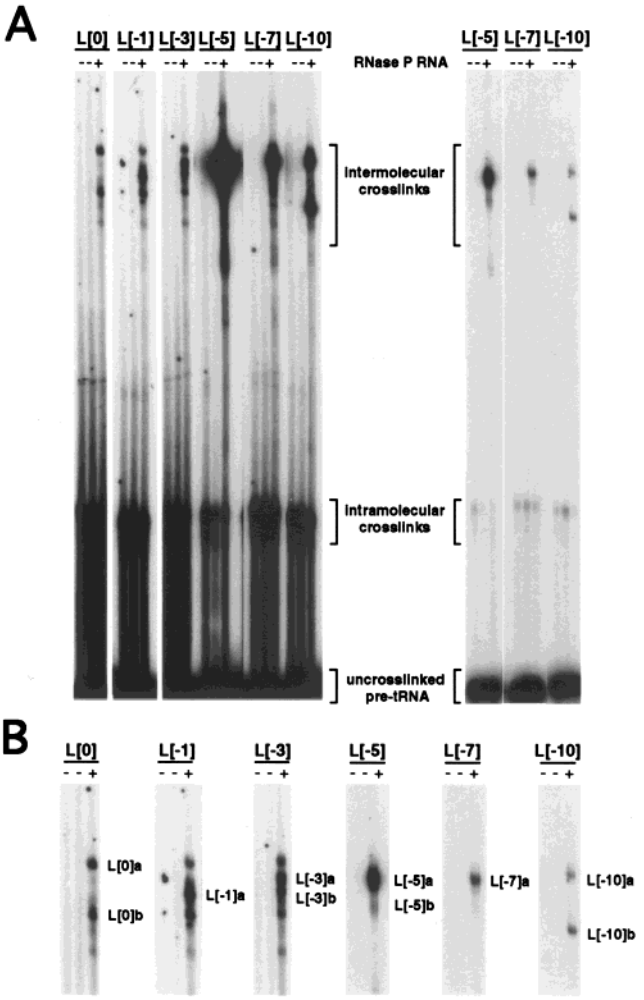

FIGURE 3: Intermolecular cross-linking between 5′ end-labeled s^{4}U-modified pre-tRNA and RNase P RNA. (A) The pre-tRNAs used in the cross-linking reactions as well as the presence (+) or absence (−) of RNase P RNA are indicated above each lane. The positions of un-cross-linked pre-tRNA, intramolecular cross-links of pre-tRNAs, and intermolecular cross-linked species are indicated by brackets adjacent to the autoradiograms. A shorter exposure of the lanes containing L[−5], L[−7], and L[−10] RNAs is shown at the right. (B) Identification of individual intermolecular cross-linked species. The portion of the gel containing intermolecular cross-links in part A is shown. The designations for each of the individual intermolecular cross-linked species are shown to the right of each autoradiogram.

s^{4}U at Different Positions in the Pre-tRNA 5′ Leader Cross-links to Discrete Elements of the RNase P Ribozyme Structure. Primer extension mapping was used to confirm that the cross-links were indeed intermolecular and to determine the location of the cross-links on both the pre-tRNA substrates and the *B. subtilis* ribozyme. Individual cross-linked species were isolated by gel purification and used as substrates for in vitro transcription with reverse transcriptase, which terminates one nucleotide prior to cross-

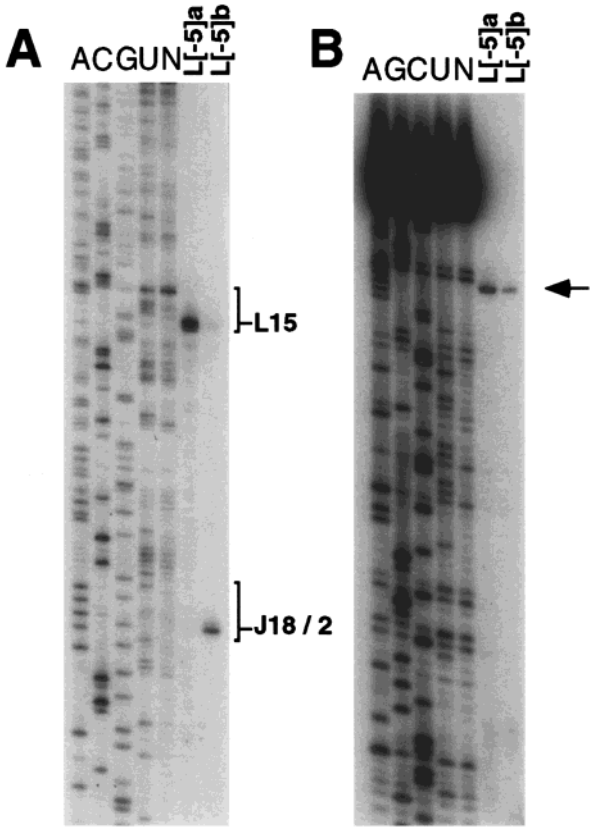

FIGURE 4: Cross-linking and primer extension mapping of cross-linked species derived using the L[−5] pre-tRNA. (A) Primer extension mapping of cross-linked nucleotides in RNase P RNA. Lanes marked L[−5]a and L[−5]b contain extension products from the corresponding cross-linked species. Lanes marked N, A, G, C, and U contain extension products from un-cross-linked RNA or reverse transcriptase dideoxy sequencing standards, respectively. The regions of RNase P RNA secondary structure referred to in the text to which cross-link-specific terminations were mapped are indicated by brackets to the right of the autoradiograms. Individual cross-linked nucleotides are given in Table 1. (B) Primer extension mapping of photoagent incorporation sites in pre-tRNA. Lanes are designated as in panel A. An arrow indicates the position of nucleotide U-5 in the primer extension sequencing products.

links in the RNA template (*22* and references therein). Comparison of the extension products obtained with the isolated cross-linked species to control reactions containing un-cross-linked RNA and dideoxy sequencing standards allowed identification of the position of the individual cross-linked nucleotides.

Primer extension mapping results for the two L[−5] specific intermolecular cross-links are shown in Figure 4. The cross-linked species with slowest mobility was given the designation L[−5]a and the faster mobility species was designated L[−5]b (see Figure 3B). For the L[−5]a species cross-linking occurs to nucleotides G258 and G259 in L15 of the *B. subtilis* ribozyme (Figure 4A). In contrast, the L[−5]b species results from cross-linking to a different region of the ribozyme. Here, specific primer extension terminations demonstrate cross-linking to nucleotide A320 in J18/2. To confirm that the intermolecular cross-linking resulted from incorporation of a s^4U at position −5 in the leader sequence, a corresponding analysis on the same RNA sample was performed using oligonucleotide primers specific for tRNA sequences (Figure 4B). As expected, primer extension terminates one nucleotide 3′ to position −5 in the 5′ leader sequence, demonstrating that both the L[−5]a and L[−5]b intermolecular cross-links involved s^4U residues at position −5.

Primer extension analyses of the L[−1], L[−3], L[−7], and L[−10] specific intermolecular cross-links are shown in Figure 5, and the results are summarized in Table 1. We find that these cross-linked species resulted from cross-linking between the unique uridines in the 5′ leader sequence and four different regions of ribozyme structure. Cross-linked species with similar mobilities on denaturing gels were found to result from cross-linking to the same general region of the ribozyme. L[−1]a and L[−3]b result from cross-linking to nucleotides (U317, A318, and G319) in the J18/2 element of *B. subtilis* RNase P RNA adjacent to that identified in band L[−5]b (Figure 5 and Table 1), consistent with the similar mobility of these three cross-linked species in denaturing gel electrophoresis (Figure 3). Similarly, L[−7]a results from cross-linking to G259, U260, and A261 in L15, and L[−10]a contains cross-links to nucleotides G258−A261 in the same region of the ribozyme. Again, these results are consistent with the similar mobilities of bands L[−5]a, L[−7]a, and L[−10]a with respect to one another in denaturing gels (Figure 3). Band L[−3]a resulted from cross-linking to an adjacent region in the ribozyme at A245 and A246 within J5/15 and ran slightly faster than bands L[−5]a, L[−7]a, and L[−10]a. Finally, species L[−10]b had the fastest mobility in denaturing gels and resulted from cross-linking to a more distal region of the ribozyme, nucleotides A36 and U37 in P3 of the *B. subtilis* ribozyme secondary structure (Figure 5 and Table 1).

Importantly, sites of cross-linking to the pre-tRNA sequences were determined for each band described above and were found to involve the unique uridine residues in the 5′ leader sequence of the L[−1], L[−3], L[−5], L[−7], and L[−10] pre-tRNA substrates (Table 1 and data not shown). Cross-links in L[0]a and L[0]b could not be mapped by primer extension and produced insufficient material for fingerprint analysis. These cross-linked species likely involve uridines near the 3′ end of the tRNA sequence within the oligonucleotide binding site used for primer extension. However, for the cross-links unique to the leader sequences of the L[−1], L[−3], L[−5], L[−7], and L[−10] pre-tRNA substrates, specific primer extension terminations identified nucleotides in J5/15, J18/2, L15, and P3 as being in close proximity to the 5′ leader in the ribozyme-substrate complex.

Intermolecular Cross-Links between the Pre-tRNA 5′ Leader and RNase P RNA Retain Catalytic Activity. To address whether the cross-linked RNAs could adopt the active ribozyme conformation, the individual cross-linked species were isolated and tested for catalytic activity. Individual cross-linked species containing 5′ end-labeled pre-tRNA that were generated in the presence of calcium were gel purified and subsequently incubated in reaction buffer containing $MgCl_2$ to accelerate the cleavage reaction (Figure 6). In some reactions we observed variable amounts of RNA with mobility consistent with free pre-tRNA. These species could have resulted from the partial reversal of the s^4U cross-links or could be contaminating free pre-tRNA from gel purification. For the cross-links between RNase P RNA and the mature tRNA domain of the substrate, cleavage should release the radiolabeled 5′ leader. On the other hand, cleavage of cross-links between RNase P RNA and the 5′ leader

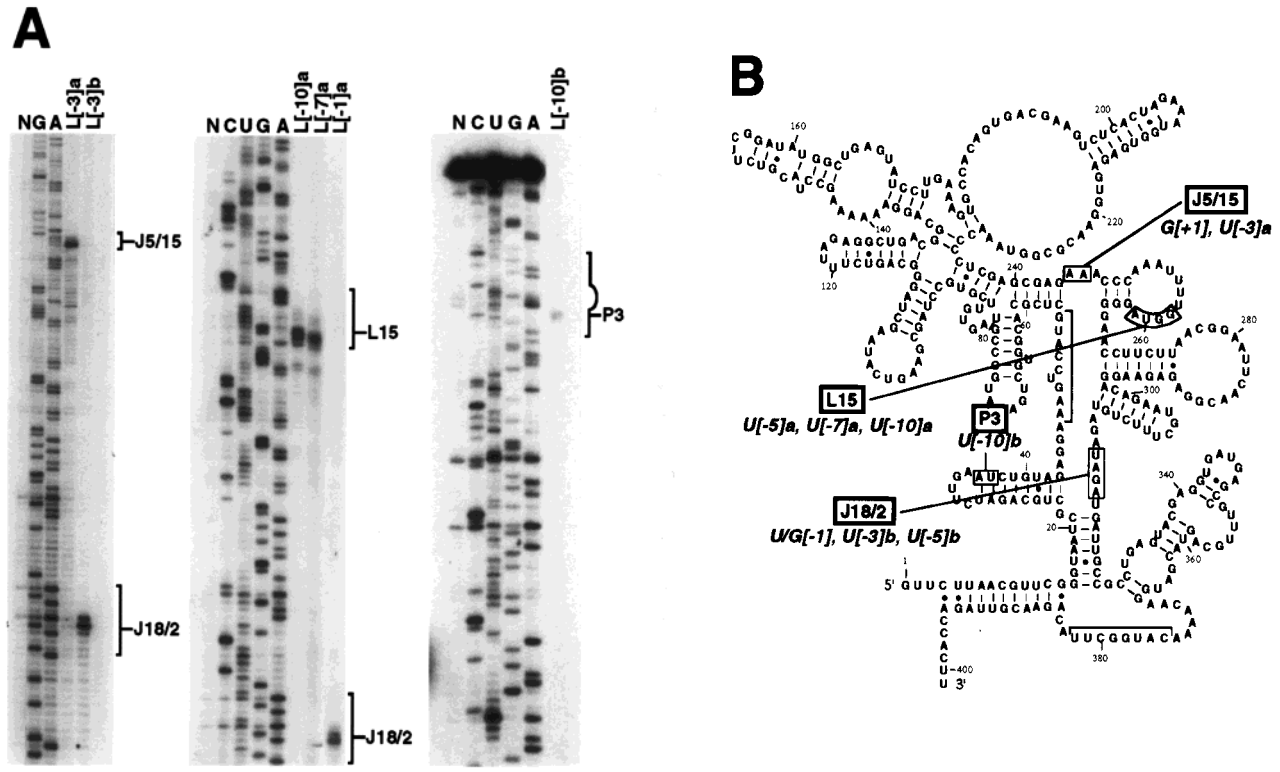

FIGURE 5: Primer extension mapping of intermolecular cross-link sites between L[−1], L[−3], L[−7], and L[−10] pre-tRNAs and RNase P RNA. (A) The individual cross-linked conjugates used as primer extension templates are designated as in Figure 3B. Lanes marked N, A, G, C, and U contain extension products from un-cross-linked RNA or reverse transcriptase dideoxy sequencing standards, respectively. The regions of RNase P RNA secondary structure referred to in the text to which cross-link-specific terminations were mapped are indicated by brackets to the right of the autoradiograms. An arc in the bracket indicating P3 shows the location of the P3 loop. (B) The nucleotide positions that were cross-linked by s^4U in the pre-tRNA 5′ leader are indicated on the secondary structure of RNase P RNA. Nucleotide positions in RNase P RNA that were sites of cross-linking are boxed and labeled with the name of the corresponding region of the RNase P RNA structure and the pre-tRNA nucleotide position (in italics) which cross-linked to that site. Nucleotide positions in tRNA are numbered relative to the mature tRNA 5′ end (e.g., G[+1] is the first nucleotide in the mature tRNA sequence, and U[−3] is in the leader sequence, three nucleotides upstream of the mature tRNA 5′ end).

should release the nonradiolabeled tRNA, and the radiolabeled 5′ leader should remain covalently associated with the ribozyme. Cross-links from the control substrate L[0] which contains no uridine residues in the 5′ leader sequence are predicted to reside within the mature tRNA domain. Indeed, upon incubation of the L[0]a and L[0]b cross-linked species with magnesium, the end-labeled 5′ leader fragment was released from the conjugate. In contrast, when the cross-linked conjugates involving uridine residues in the 5′ leader sequences of the L[−1], L[−3], L[−5], L[−7], and L[−10] pre-tRNAs were incubated with magnesium, no end-labeled 5′ leader fragment was released from the conjugate, but rather a fragment is produced with a mobility similar to that of the un-cross-linked ribozyme, consistent with cleavage and the loss of the unlabeled mature tRNA domain. Thus, the products of the cleavage reactions of the cross-linked conjugates provide additional evidence that the cross-linked species specific to the L[−1], L[−3], L[−5], L[−7], and L[−10] pre-tRNAs result from cross-linking to the 5′ leader. Importantly, these data demonstrate that the individual cross-linked species retain significant catalytic activity, which strongly suggests, but does not directly prove, that the cross-links occurred within the native structure of the ribozyme−substrate complex. Taken together, the data presented here show that different positions along the 5′ leader are associated with discrete regions of the ribozyme, including J5/15, J18/2, L15, and P3 in the active ribozyme−substrate complex.

DISCUSSION

Photo-cross-linking, biochemical, and kinetic studies have provided significant insight into the recognition of the mature tRNA domain of the pre-tRNA substrate by the RNase P ribozyme. In contrast, the recognition of the 5′ leader and its location in the ribozyme−substrate complex are less well understood. In previous studies, we examined short-range photo-cross-linking of bases at, or immediately adjacent to, the cleavage site (*26*). Consistent with other biochemical and cross-linking studies (*14, 22, 24*), we found that the nucleotide base immediately upstream of the cleavage site in a substrate with a single nucleotide leader was proximal (<3 Å) to the highly conserved single-stranded region J18/2 in both *Escherichia coli* and *B. subtilis* RNase P RNAs. To examine whether pre-tRNAs with longer 5′ leaders are positioned similarly within the enzyme−substrate complex and to determine the local three-dimensional environment of the 5′ leader, we examined short-range cross-linking from the 5′ leader using the photoaffinity reagent s^4U. In this analysis we report a series of specific photo-cross-links between individual nucleotides in the 5′ leader sequence of pre-tRNA and specific elements of the *B. subtilis* RNase P ribozyme.

The data presented here show that the nucleotide at position −1 in the pre-tRNA leader sequence is adjacent to nucleotides A318 and G319 in the J18/2 region of the *B.*

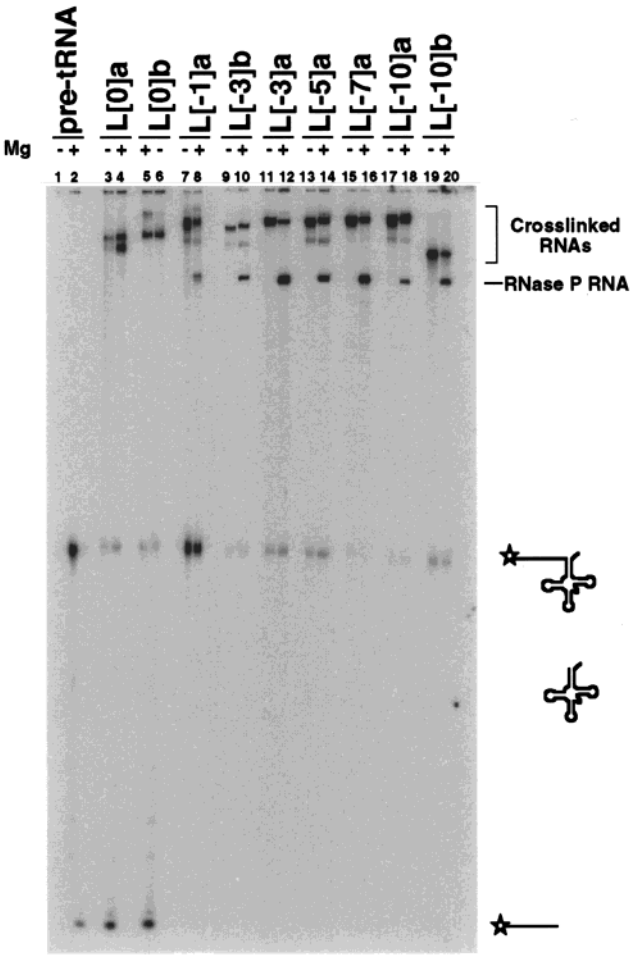

FIGURE 6: Catalytic activity of intermolecular cross-linked species. Individual cross-linked species from preparative reactions performed in the presence of calcium were gel purified and subsequently incubated in reaction buffer in the presence of magnesium. The identity of the specific cross-linked species and the presence (+) or absence (−) of magnesium in the reaction are indicated above each lane. The relative mobility of the cross-linked conjugates, uncross-linked RNase P RNA, pre-tRNA, mature tRNA, and the 5′ leader fragment are shown to the right of the autoradiogram.

subtilis ribozyme. These nucleotide positions were also detected using 6-thioguanosine at position −1 in the context of a pre-tRNA with only a single nucleotide leader sequence, demonstrating that the proximity of the −1 position to J18/2 is not idiosyncratic to any particular photoagent or leader sequence length (*26*). The presence of a longer 5′ leader, however, shifts the position of the major site of cross-linking by one nucleotide in J18/2 from A318 to G319, suggesting that the additional 5′ leader nucleotides may influence the location of the base immediately upstream of the cleavage site. Indeed, Fierke and co-workers observed, under conditions of low ionic strength, that increasing the length of the 5′ leader from one to just two nucleotides increases the ground-state binding of the substrate in both *B. subtilis* RNase P RNA and the holoenzyme by 8-fold and 160-fold, respectively (*43*). Ground-state binding of pre-tRNA substrates by *B. subtilis* RNase P RNA, however, is increased significantly under conditions of high ionic strength and is, in fact, equivalent to that of the holoenzyme for substrates containing a two nucleotide leader, suggesting the potential involvement of direct RNA−RNA contacts with the 5′ leader sequence (*43*). Significant changes in the pattern of accessibility of J18/2 to chemical modification are also observed in the presence of pre-tRNA but not when tRNA is bound to the ribozyme (*14*). For the *B. subtilis* RNase P RNA, substrates with 5′ leaders as short as two nucleotides are sufficient to protect position G319 from kethoxal, which modifies the base-pairing edge of the nucleotide base. The current work thus provides further support for the conclusion that the J18/2 element of ribozyme structure is proximal to the 5′ leader and that contacts which may play a direct role in positioning the leader in the ribozyme−substrate complex are likely to reside immediately upstream of the cleavage site.

Cross-linking to J18/2 is also observed when s^4U is incorporated at positions −3 and −5 of the 5′ leader sequence (Table 1). The presence of similar cross-links from the −3 to −5 region of the 5′ leader may, therefore, reflect a high degree of susceptibility of J18/2 to nucleophilic attack or structural flexibility within the ribozyme−substrate complex. However, movement of the cross-linking agent just two nucleotides upstream from position −3 to position −5 results in a dramatic decrease in cross-linking to J18/2 and a highly efficient cross-link to a new region of the *B. subtilis* ribozyme, L15 (Figures 5 and 7B). Movement of the cross-linking agent two nucleotides further upstream to position −7 results in cross-linking uniquely to L15 while movement of the cross-linking agent an additional three nucleotides upstream to position −10 results in roughly equal levels of cross-linking to L15 and a third region of the ribozyme, P3 (Figures 3 and 7B).

Cross-linking of the 5′ leader to L15 is of particular interest because this portion of the ribozyme is also known to be involved in binding the conserved 3′ CCA sequence of pre-tRNA (*14*−*16*). The current cross-links are therefore consistent with the general position of L15 at the base of the pre-tRNA acceptor stem (*22*, *24*, *25*). The short-range (<3 Å) cross-links from positions −5, −7, and −10, however, do not necessarily imply direct interactions with the L15 region but minimally the relative position of L15 with respect to different nucleotide positions along the 5′ leader. Consistent with these data, long-range (±9 Å) cross-linking experiments with azidophenacyl reagents recently showed that L15 is adjacent to both J18/2 and L3 in both the *E. coli* and *B. subtilis* ribozymes, indicating that the proximity of these three regions of the ribozyme is a general feature of bacterial RNase P RNA structure (*25*, *33*). The current work, therefore, builds upon the previous long-range cross-linking studies by further defining the relative positions of J18/2, L15, and L3. These structural constraints provide an important addition to theoretical models of the ribozyme−substrate complex, which either lack the 5′ leader (*25*) or position the 5′ leader only on the basis of structural constraints of bases immediately upstream of the cleavage site (*34*).

Taken together, these data indicate that the 5′ leader sequentially passes through three discrete regions of the *B. subtilis* ribozyme. Using the cross-linking data presented here and in previous studies (*24*−*26*, *33*), we propose the following position for the pre-tRNA 5′ leader (illustrated in Figure 7). In the ground-state ribozyme−substrate complex, the pre-tRNA cleavage site is flanked by J5/15 and J18/2, with the conserved adenosines in J5/15 located proximal to the mature tRNA 5′ end. J18/2 is adjacent to nucleotides just upstream of the cleavage site (positions −1 to −3) and

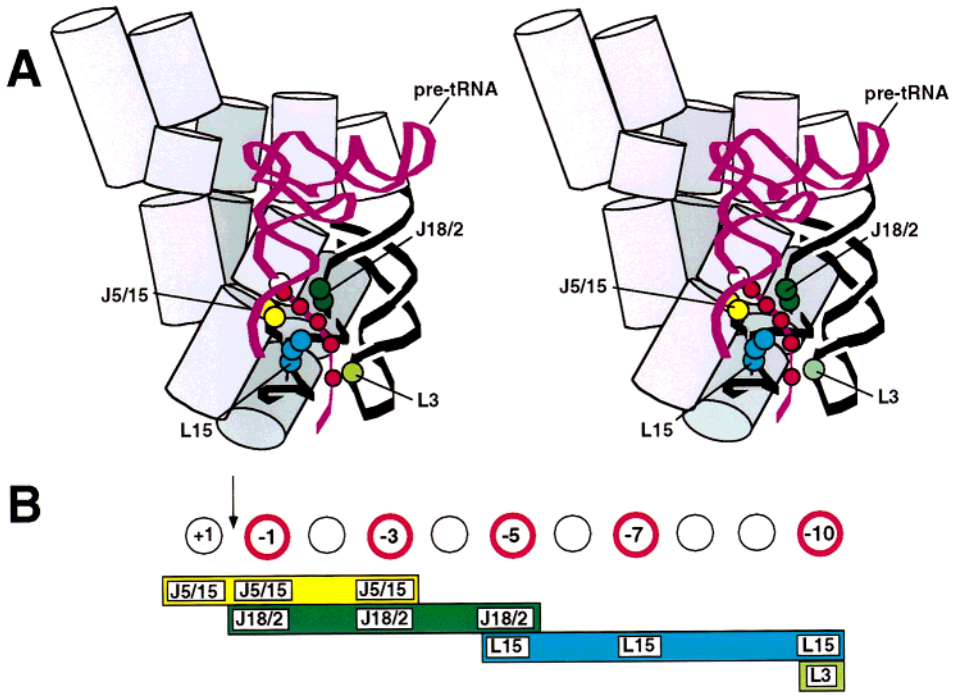

FIGURE 7: Summary of intermolecular cross-linking results between the pre-tRNA 5′ leader and the RNase P ribozyme. (A) Track of the 5′ leader in the ribozyme−substrate complex. The position and orientation of helices in the *B. subtilis* ribozyme are indicated by cylinders. The path of the phosphodiester backbone of pre-tRNA and helices P2, P3, and P15 of RNase P RNA are shown as purple and black ribbons, respectively. The locations of s^4U incorporation sites and cross-linked nucleotides on RNase P RNA are shown as red spheres. Structure elements of RNase P RNA detected by cross-linking to the 5′ leader are shown as spheres that are colored according to part B. (B) Schematic diagram of regions of RNase P RNA adjacent to the 5′ leader. Elements of ribozyme structure detected in intermolecular cross-linking experiments are indicated below the appropriate nucleotide.

may play a direct role in binding functional groups in the 5′ leader. Interestingly, we find that the nucleotides at positions −5 to −10 in the leader are adjacent to the 3′ CCA binding site in L15. Finally, as might be expected, the most distal portion of the 5′ leader is located in peripheral, phylogenetically variable elements of structure in helix P3.

Given recent evidence that the RNase P protein subunit makes contact with the distal portion of the 5′ leader (*31*, *32*), it is tempting to speculate that the region of ribozyme structure that binds the protein subunit overlaps with the regions identified here. Chemical protection and hydroxy radical footprinting studies in *E. coli* RNase P have suggested the interaction of the protein subunit with numerous regions of the ribozyme (*44*−*46*); however, the precise binding site of the RNase P protein on RNase P RNA remains unclear. Kinetic analysis of the cleavage of substrates with various leader lengths by *B. subtilis* RNase P indicates a likely contact between the protein subunit and the 5′ leader (*31*, *43*). In addition, long-range (9 Å) cross-links between the P protein and leader sequences −4 to −8 have been reported (*32*). The short stretch of three nucleotides between the cleavage site and the site of protein binding provides a significant distance constraint on the position of the protein in structures of the ribozyme−substrate complex. This constraint places the protein subunit immediately adjacent to J18/2, L15, and P3 where we observe efficient and unambiguous cross-linking from positions −5 to −10 in the 5′ leader in *B. subtilis* RNase P RNA. Consistent with these observations, experiments using an Fe-EDTA reagent tethered to *E. coli* C5 protein result in a discrete region of reactivity in helix P3 (V. Gopalan, personal communication). Taken together, these data suggest that the position of the 5′ leader along the surface of the ribozyme may be indicative of its position within the holoenzyme−substrate complex.

In summary, we have examined the track of the 5′ leader in the ribozyme−substrate complex. The short-range intermolecular cross-linking between nucleotides proximal to the cleavage site and J18/2 is consistent with a variety of biochemical and structural data, and the present observations help to orient the 5′ leader with respect to this element of ribozyme structure. In particular, the positional data reported here provide new insight into the relative orientation of the 5′ leader and ribozyme by suggesting that the 5′ leader is positioned along a surface that includes the CCA binding site in L15 and a peripheral element of ribozyme structure, P3. The short-range cross-linking approach outlined here should also be applicable to the holoenzyme, and future efforts along these lines can address whether the RNase P protein influences the position of the 5′ leader relative to the catalytic RNA subunit.

ACKNOWLEDGMENT

We gratefully acknowledge the help and advice of Dr. Craig Peebles and Dr. David McPheeters. We are indebted to Dr. Norman Pace for providing materials in the initial stages of this study and for advice and encouragement. We thank Dr. Jonatha Gott, Nathan Zahler, Nicholas Kaye, Adam Cassano, Frank Campbell, and Dr. Jo Ann Wise for advice and comments of the manuscript.

REFERENCES

1. Altman, S., and Kirsebom, L. (1999) in *The RNA World* (Gesteland, R. F., Cech T. R., and Atkins, J. F., Eds.) pp 351−

380, Cold Spring Harbor Laboratory Press, Cold Spring Harbor, NY.
2. Frank, D. N., and Pace, N. R. (1998) *Annu. Rev. Biochem. 67*, 153−180.
3. Guerrier-Takada, C., Gardiner, K., Marsh, T., Pace, N., and Altman, S. (1983) *Cell 35*, 849−857.
4. Cech, T. R., and Golden, B. L. (1999) in *The RNA World* (Gesteland, R. F., Cech T. R., and Atkins, J. F., Eds.) pp 321−349, Cold Spring Harbor Laboratory Press, Cold Spring Harbor, NY.
5. McClain, W. H., Guerrier-Takada, C., and Altman, S. (1987) *Science 238*, 527−530.
6. Kirsebom, L. A., and Svard, S. G. (1992) *Nucleic Acids Res. 20*, 425−432.
7. Svard, S. G., and Kirsebom, L. A. (1992) *J. Mol. Biol. 227*, 1019−1031.
8. Svard, S. G., and Kirsebom, L. A. (1993) *Nucleic Acids Res. 21*, 427−434.
9. Holm, P. S., and Krupp, G. (1992) *Nucleic Acids Res. 20*, 421−423.
10. Gaur, R. K., and Krupp, G. (1993) *Nucleic Acids Res. 21*, 21−26.
11. Pan, T., Loria, A., and Zhong, K. (1995) *Proc. Natl. Acad. Sci. U.S.A. 92*, 12510−12514.
12. Loria, A., and Pan, T. (1997) *Biochemistry 36*, 6317−6325.
13. Loria, A., and Pan, T. (1998) *Biochemistry 37*, 10126−10133.
14. LaGrandeur, T. E., Hüttenhofer, A., Noller, H. F., and Pace, N. R. (1994) *EMBO J. 13*, 3945−3952.
15. Oh, B.-K., and Pace, N. R. (1994) *Nucleic Acids Res. 22*, 4087−4094.
16. Kirsebom, L. A., and Svard, S. G. (1994) *EMBO J. 13*, 4870−4876.
17. Oh, B.-K., Frank, D. N., and Pace, N. R. (1998) *Biochemistry 37*, 7277−7283.
18. Hardt, W. D., Warnecke, J. M., Erdmann, V. A., and Hartmann, R. K. (1995) *EMBO J. 14*, 2935−2944.
19. Hardt, W.-D., Erdmann, V. A., and Hartmann, R. K. (1996) *RNA 2*, 1189−1198.
20. Heide, C., Pfeiffer, T. Nolan, J. M., and Hartmann, R. K. (1999) *RNA 5*, 102−116.
21. Siew, D., Zahler, N. H., Cassano, A. G., Strobel, S. A., and Harris, M. E. (1999) *Biochemistry 38*, 1873−1883.
22. Burgin, A. B., and Pace, N. R. (1990) *EMBO J. 9*, 4111−4118.
23. Nolan, J. M., Burke, D. H., and Pace, N. R. (1993) *Science 261*, 762−765.
24. Harris, M. E., Nolan, J. M., Malhotra, A., Brown, J. W., Harvey, S. C., and Pace, N. R. (1994) *EMBO J. 13*, 3953−3963.
25. Chen, J.-L., Nolan, J. M., Harris, M. E., and Pace, N. R. (1998) *EMBO J. 17*, 1515−1525.
26. Christian, E. L., McPheeters, D. S., and Harris, M. E. (1998) *Biochemistry 37*, 17618−17628.
27. Odell, L., Huang, V., Jakacka, M., and Pan, T. (1998) *Nucleic Acids Res. 26*, 3717−3723.
28. Harris, M. E., and Pace, N. R. (1995) *RNA 1*, 210−218.
29. Frank, D. N., Ellington, A. E., and Pace, N. R. (1996) *RNA 2*, 1179−1188.
30. Frank, D. N., and Pace, N. R. (1997) *Proc. Natl. Acad. Sci. U.S.A. 94*, 14355−14360.
31. Kurz, J. C., Niranjanakumari, S., and Fierke, C. A. (1998) *Biochemistry 37*, 2393−2400.
32. Niranjanakumari, S., Stams, T., Crary, S. M., Christianson, D. W., and Fierke, C. A. (1998) *Proc. Natl. Acad. Sci. U.S.A. 95*, 15212−15217.
33. Harris, M. E., Kazantsev, A. V., Chen, J. L., and Pace, N. R. (1997) *RNA 3*, 561−576.
34. Massire, C., Jaeger, L., and Westhof, E. (1998) *J. Mol. Biol. 279*, 773−793.
35. Beebe, J. A., and Fierke, C. A. (1994) *Biochemistry 33*, 10294−10304.
36. Smith, D., Burgin, A. B., Haas, E. S., and Pace, N. R. (1992) *J. Biol. Chem. 267*, 2429−2436.
37. Wetzel, R., and Soll, D. (1977) *Nucleic Acids Res. 4*, 1681−1694.
38. Barritault, D., Buckingham, R. H., Favre, A., and Thomas, G. (1981) *Biochimie 63*, 587−593.
39. Sontheimer, E. J. (1994) *Mol. Biol. Rep. 20*, 35−44.
40. Favre, A., Saintome, C., Fourrey, J. L., Clivio, P., and Laugaa, P. (1998) *J. Photochem. Photobiol. 42*, 109−124.
41. Dawson, R. M. C., Elliot, D. C., Elliot, W. H., and Jones, K. M. (1995) *Data for Biochemical Research*, Oxford Science Publications, Oxford University Press, Oxford, U.K.
42. Komine, Y., Adachi, T., Inokuchi, H., and Ozeki, H. (1990) *J. Mol. Biol. 212*, 579−598.
43. Crary, S. M., Niranjanakumari, S., and Fierke, C. A. (1998) *Biochemistry 37*, 9409- 9416.
44. Talbot, S. J., and Altman, S. (1994) *Biochemistry 33*, 1406−1411.
45. Westhof, E., Wesolowski, D., and Altman, S. (1996) *J. Mol. Biol. 258*, 600−613.
46. Kim, J. J., Kilani, A. F., Zhan, X., Altman, S., and Liu, F. (1997) *RNA 3*, 613−623.
47. Haas, E. S., Brown, J. W., Pitulle, C., and Pace, N. R. (1994) *Proc. Natl. Acad. Sci. U.S.A. 91*, 2527−2531.

BI991278A